

Modeling and optimization of biosorption of lead (II) ions from aqueous solution onto pine leaves (*Pinus kesiya*) using response surface methodology

Phuong-Thao Huynh^a, Ngoc-Tuan Nguyen^b, Ha Nguyen Van^a, Phuong-Tung Nguyen^{c,d}, Trinh Duy Nguyen^e, Van-Phuc Dinh^{f,*}

^aDepartment of Chemistry, DaLat University, 01 Phu Dong Thien Vuong St., Dalat, Vietnam, emails: thaohp@dlu.edu.vn (P.T. Huynh), hanv@dlu.edu.vn (H.N. Van)

^bNuclear Research Institute, 01 Nguyen Tu Luc, Dalat city, Lam Dong, Vietnam, email: ngoctuan45nri@gmail.com

^cCIRTECH Institute, Ho Chi Minh City University of Technology (HUTECH), Vietnam, 475A Dien Bien Phu, W 25, Dist Binh Thanh, HCM City, Vietnam, email: phuongtungng@gmail.com

^dInstitute of Applied Materials Science (IAMS) - VAST, Vietnam

^eCenter of Excellence for Green Energy and Environmental Nanomaterials, Nguyen Tat Thanh University, Ho Chi Minh City, Vietnam, email: ndtrinh@ntt.edu.vn

^fFuture Materials and Devices Laboratory, Institute of Fundamental and Applied Sciences, Duy Tan University, 10C, Tran Nhat Duat, District 1, Ho Chi Minh City, 700000, Vietnam, Tel. +84909442342; email: dinhvanphuc@duytan.edu.vn

Received 4 April 2019; Accepted 23 August 2019

ABSTRACT

In this work, the central composite design in response surface methodology by the Design-Expert software was used for optimizing the removal of Pb(II) ions from aqueous solution by pine leaves (*Pinus kesiya*). Effects of pH_{solution}, adsorption time and initial Pb(II) ions concentration on adsorption capacity were investigated. Experimental data were fitted by using five nonlinear isotherm models including Langmuir, Freundlich, Sips, Temkin and Dubinin–Radushkevich. The maximum Pb(II) adsorption capacity (q_{max}) estimated from the Langmuir isotherm model was 31.04 mg/g, which is higher than other biomaterials such as barley straw, *Cucumis sativus* peel, coconut tree sawdust, etc. Kinetic studies indicated that the uptake of Pb(II) occurred on the Elovich model within two stages. Thermodynamic studies at different temperatures showed the biosorption to be endothermic and spontaneous. The study concluded that *P. kesiya* can be a good adsorbent for removing Pb(II) from aqueous solution.

Keywords: Response surface methodology (RSM); *Pinus kesiya*; Adsorption; Isotherm; Kinetics

1. Introduction

Nowadays, the industrialization leads to an increase in environmental pollution, especially organic compounds and heavy toxic metals released from industrial zones. Among them, Pb(II) affects human health causing serious illness, such as anemia, encephalopathy, and hepatitis [1]. Thus, a great deal of physicochemical, biological, chemical methods

have been used to remove heavy toxic metals from wastewater, in which biosorption is a promising method because of its low cost and high efficiency. However, the efficiency of the removal depends on many factors, such as pH, adsorption time and initial concentration. This leads to a large number of tests which needs to be determined before applying to environmental treatment. Nevertheless, a number of experiments can be reduced by using optimization tools. In recent

* Corresponding author.

years, response surface methodology (RSM) which includes a group of a mathematical algorithm and statistical techniques has been largely applied to minimize the number of experiments, thus reducing a large number of chemicals and time-consuming processes [2–5]. It means that this method will provide an equation to evaluate the relationship between a group of controlled experimental factors and measured responses based on one or more criteria. In addition, it can be utilized to evaluate the effects of individual parameters, the interaction of variables, and the optimum conditions for responses.

There are many bioadsorbents sourced from locally available natural materials which have been used to replace expensive adsorbent materials, such as corn cobs, banana peel and sawdust [6,7]. *Pinus kesiya*, which has been popularly planted in South-East Asia, can be utilized for a variety of applications, including boxes, paper pulp and temporary electric poles [8,9]. However, the use of *Pinus kesiya* as a biological, cheap, easy-going and environmental friendly material to remove Pb(II) from aqueous solution has not been widely interested. In the present study, the experimental factorial design and RSM with central composite design (CCD) under Design-Expert software [10] was used to optimize the removal of lead (II) ions from aqueous solution by *Pinus kesiya* leaves. Factors affecting the adsorption, such as pH_{solution}, contact time and initial concentration will be studied. Isotherm and kinetic models were used to estimate the capacity and mechanism of the adsorption.

2. Materials and methods

2.1. Preparation of adsorbent

The fallen pine leaves used in this study were collected from Dalat city of Vietnam. They are needle-like and dark brown (Fig. 1). They were thoroughly cleaned to remove dust and dirt by soaking them with clean water for 1 d and then rinsing with distilled water until the wash water was not opaque. The pine leaves were cut to about 2 cm, dried at 80°C to obtain a constant weight (24 h), then crushed and sieved to the following size: $125 \mu\text{m} < d \leq 212 \mu\text{m}$. The material was stored in airtight plastic containers at room temperature [11].

2.2. Chemicals and instruments

All chemicals used in the present work were of analytical grade. 1,000 mg/L standard stock solution of Pb(II) ions.



Fig. 1. Pine leaves collected from Dalat city of Vietnam.

The pH of the solutions was adjusted by using 0.1 M HNO₃ and 0.1 M NaOH solutions.

In order to examine the morphology of the pine leaves, the FESEM Hitachi S-4800 (made by Hitachi, Japan) is utilized. Additionally, the material bonding before and after the uptake is determined within the Fourier transform infrared spectroscopy using Nicolet iS5 (made by Thermo Scientific, USA).

2.3. Experiments

The batch adsorption experiments were carried out by contacting 0.5 g of adsorbent with 50 mL of metal ions solutions in the sealed 100 mL flasks. The suspensions were magnetically stirred at 240 rpm at room temperature (25°C). Factors affecting the adsorption, such as pH 2–6, adsorption time 10–240 min and initial concentration 50–300 mg/L, were examined. After the specified time, suspensions were filtered through filter paper with 0.65 μm of pore size. Concentrations of Pb(II) ions in the filtrates were determined by Shimadzu Atomic Absorption Spectrometry AA – 6800 Series (Japan).

In all the cases, the adsorption capacity q (mg/g) and the adsorption efficiency $A\%$ were calculated as follows [1]:

$$q_e = \frac{(C_0 - C_e) \times V}{m} \quad (1)$$

$$A\% = \frac{(C_0 - C_e) \times 100\%}{C_0} \quad (2)$$

where q_e is the adsorption capacity (mg/g) at equilibrium, C_0 and C_e are the initial concentration and the equilibrium concentration of Pb(II) ions (mg/L), respectively. V is the volume (L) of the solution and m is the mass of adsorbent used (g).

2.4. Experimental design and analysis with RSM

In this work, RSM with CCD was chosen to optimize three independent factors: pH, adsorption time and initial Pb(II) concentration, which mainly affect the Pb(II) adsorption. The total number of experiments was generated using the following equation [12]:

$$N = 2^k + 2.k + 6 = 2^3 + 2.3 + 6 = 20 \quad (3)$$

where k is the number of factors and C is the number of central points.

The CCD is carried out based on the two-level factorial designs augmented with the center and axial points to fit the quadratic models. In this work, the CCD is made up of three factors, each at five levels ($-\alpha, -1, 0, +1, +\alpha$; Table 1). Here, the ± 1 codes are used to define the limits for the area of interest where the optimum is believed to exist, whereas the 0 code corresponds to the center level which is in the middle of the lowest and highest levels. The $\pm\alpha$ codes are chosen in order to ensure that the extreme axial runs are within the area of operability. The adsorption capacity,

Table 1
Experimental range and coded levels of the selected process variables

| Variable (factors) | Coded levels | | | Star points ($\alpha = 1.68$) | |
|---|--------------|-------------|--------------|---------------------------------|-----------|
| | Lowest (-1) | Central (0) | Highest (+1) | $-\alpha$ | $+\alpha$ |
| pH (A) | 4 | 5 | 6 | 3.32 | 6.68 |
| Time (B), min | 70 | 90 | 110 | 56 | 124 |
| Initial concentration (C), mg L ⁻¹ | 170 | 190 | 210 | 156 | 224 |

which is related to a number of independent variables, can be expressed by the following quadratic model [2,12]:

$$Y = \beta_0 + \sum_{i=1}^k \beta_i \cdot x_i + \sum_{i=1}^k \sum_{j=1}^k \beta_{ij} x_i x_j + \sum_{i=1}^k \beta_{ii} x_i^2 \quad (4)$$

where y is the predicted response (Pb(II) adsorption capacity), β_0 is the constant coefficient, x_i ($i = 1-3$) are three parameters being studied (pH, time and initial concentration), and β_i , β_{ij} and β_{ii} are the linear, quadratic and interaction coefficients, respectively (see Section 3.3 for more details).

2.5. Isotherm and kinetic models

The experimental data were fitted by using five non-linear models including Langmuir, Freundlich, Sips, Temkin and Dubinin–Radushkevich together with four nonlinear

kinetic models, namely pseudo-first-order, pseudo-second-order, Elovich and intra-diffusion models. These models are presented in Table 2 [1,13,14].

To identify the best-fit model for the adsorption process, the Chi-square (χ^2) and the coefficient of determination (R^2) of the non-linear optimization method were determined as the following equations [13,15]:

$$R^2 = 1 - \frac{\sum_{n=1}^n (q_{e,meas} - q_{e,calc})^2}{\sum_{n=1}^n (q_{e,meas} - q_{e,calc})^2} \quad (5)$$

$$\chi^2 = \sum_{n=1}^n \frac{(q_{e,meas} - q_{e,calc})^2}{q_{e,calc}} \quad (6)$$

Table 2
Isotherm and kinetics models

| Models | | Nomenclature |
|----------------------|--|--|
| Langmuir | $q_e = \frac{q_m \times K_L \times C_e}{1 + K_L \times C_e}$ | q_e (mg g ⁻¹): amount of adsorbate in the adsorbent at equilibrium C_e (mg L ⁻¹): concentration at equilibrium |
| Freundlich | $q_e = K_F \times C_e^{\frac{1}{n}}$ | Q_m (mg g ⁻¹): the maximum adsorption capacity of the adsorbent. K_L (L mg ⁻¹): the Langmuir adsorption constant. K_F : Freundlich isotherm constant (mg/g) related to adsorption capacity n : adsorption intensity |
| Sips | $q_e = \frac{Q_S \times C_e^{\beta_S}}{1 + \alpha_S \times C_e^{\beta_S}}$ | Q_S (L g ⁻¹): Sips constant α_S (L mg ⁻¹): α_S is Sips isotherm model constant β_S : Sips isotherm model exponent |
| Temkin | $q_e = \frac{RT}{b_T} \ln(k_T C_e)$ | b_T (kJ mol ⁻¹): heat of the sorption K_T : Temkin isotherm constant |
| Dubinin–Radushkevich | $q_e = Q_{D-R} \times e^{(-\beta \epsilon^2)}$ | Q_{D-R} : Dubinin–Radushkevich isotherm constant ϵ : Dubinin–Radushkevich isotherm constant β (mol ² kJ ⁻²): Dubinin–Radushkevich isotherm constant |
| Pseudo-first order | $q_t = q_e (1 - e^{-k_1 t})$ | q_t (mg g ⁻¹): amount of adsorbate in the adsorbent at any time t . k_1 (1 min ⁻¹): the rate constant of the pseudo-first-order model |
| Pseudo-second order | $q_t = \frac{q_e^2 \times k_2 \times t}{1 + k_2 \times q_e \times t}$ | k_2 (g mg ⁻¹ min): the rate constant of the pseudo-second-order model α (mg g ⁻¹ min): the rate constant of the Elovich model |
| Elovich | $q_t = \frac{1}{\beta} \ln(1 + \alpha \times \beta \times t)$ | β (mg g ⁻¹): the desorption constant during any one experiment. k_d (mg g ⁻¹ min): the rate constant of the intra-diffusion model. |
| Intra-diffusion | $q_t = k_d t^{\frac{1}{2}} + C$ | C (mg g ⁻¹): a constant describing the thickness of the boundary layer |

The smallest value of χ^2 symbol and the highest value of R^2 indicate first, a better model fit; and second, similarity of the model with the experimental data.

3. Results and discussion

3.1. Characterization of pine leaves

The scanning electron microscope (SEM) was used to characterize the morphology of pine leaves. As can be seen in the SEM images at different exaggerations shown in Figs. 2a and b, this material has a rough surface and some cavities in its structure that are favorable to the adsorption of heavy metal ions. This suggests that the biosorbent behave as structurally heterogeneous surface in the adsorption process of the Pb(II) cation. In addition, the energy-dispersive X-ray spectroscopy (EDX) depicted in Fig. 3 records the main elements of pine leaves including carbon and oxygen with 53.24% and 46.76% of weight, respectively.

In order to characterize and analyze the major functional groups that may be involved in the metal adsorption process, the FT-IR spectrum (IR) of pine leaves was measured by using the infrared spectrometer Nicolet iS5 and the obtained spectrum is shown in Fig. 4 (black line). As can be seen from this figure, the wide band at approximately $3,400\text{ cm}^{-1}$ indicates that the OH groups are stretched, whereas there is a variation of the C=O group of the carbonyl presented in the hemicellulose at $1,735\text{ cm}^{-1}$, which may be formed via undergoing the ring-opening to expose the formyl C=O functional group [16] or the oxidation of those sugars to the corresponding carboxylic functional group [17,18]. In addition, the midsection of $1,630\text{--}1,600\text{ cm}^{-1}$ shows the C=C bonding of the aromatic ring and the C=O bond. At $1,035\text{ cm}^{-1}$, the deformation of C-H and C-O bonds of cellulose, hemicellulose and lignin or C-O-C fluctuations in cellulose and hemicellulose may also be present [19].

Comparison of the pre- and after adsorption spectra reveals a decrease in intensity at $1,035\text{ to }1,061\text{ cm}^{-1}$ corresponding to the oscillations of the C-O alcoholic group, which may indicate that Pb(II) ions interact strongly with the material at this location. This finding is related to some previous reports showing details of adsorption configuration of the sugars and polyols and the insight of the interaction of C-O and O-H bonds [16,18,20].

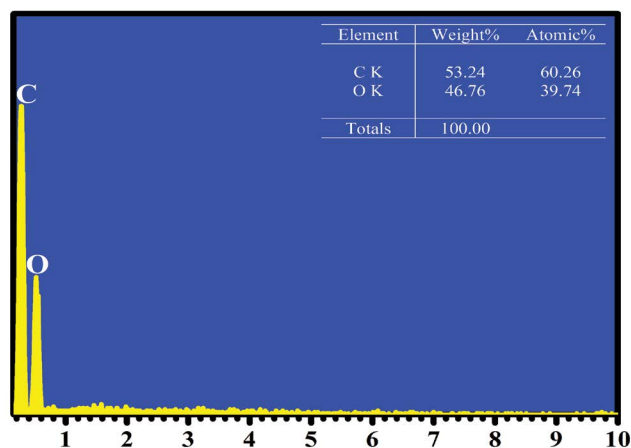


Fig. 3. EDX spectrum of pine leaves and its chemical composition.

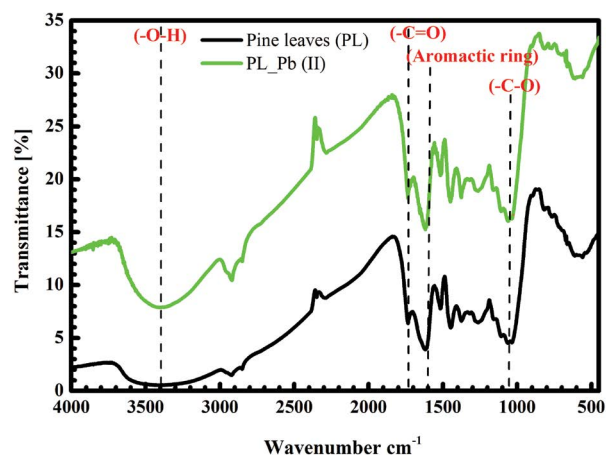


Fig. 4. Infrared spectroscopy of pine leaves before and after adsorption Pb(II).

3.2. Factors affecting the adsorption of Pb(II)

pH is one of the important factors that affects the adsorption of metal ions in aqueous solution because it impacts the charge of material's surface. If $\text{pH}_{\text{solution}}$ is smaller than

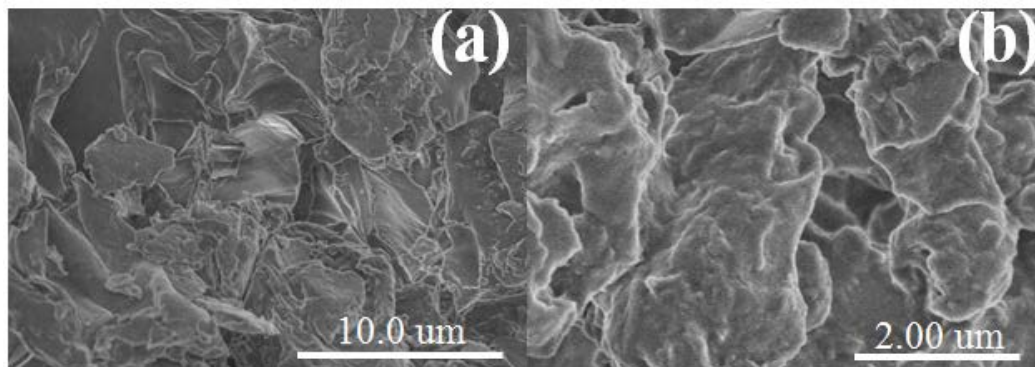


Fig. 2. SEM images of pine leaves at different exaggerations: $\times 5,000$ (a) and $\times 20,000$ (b).

pH_{pZC} value (pH_{pZC} is the pH at the point of zero charge) at which the charge of surface is zero, active sites will be positively charged and are favorable for the uptake of anions. Conversely, if $pH_{solution}$ is bigger than pH_{pZC} value, active sites will be negatively charged and be favorable to the adsorption of cations. In this work, the pH_{pZC} of pine leaves was recorded at approximately 4.5 (Fig. 5).

Fig. 6a shows the influence of pH on the adsorption of Pb(II) at the same condition. From the figure, it is apparent that the uptake of Pb(II) onto the leaves of *P. kesiyia* increases with increasing pH from 2.0 to 6.0. This can be explained by the fact that at low pH values, protons occupy the adsorption sites on the adsorbent surface and therefore less metal ions can be adsorbed because of electrostatic repulsion between the metal cations and these protons at the binding sites as shown in Eq. (7) [21].



By contrast, there is the formation of hydroxylated complexes of the metal ions at pH higher than 6.0 that compete against the metal cations at the adsorption sites [22–24]. As a result, the effective metal cations removal will be reduced. Therefore, adsorption experiments at pH above this range were not considered [25]. In this work, the maximum adsorption onto *P. kesiyia* leaves was obtained at pH 5.0 for Pb(II) with 94.80%.

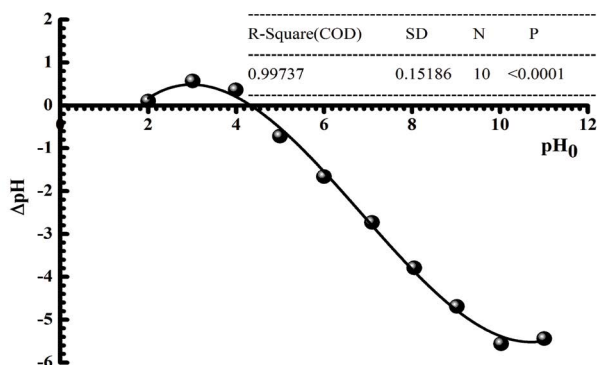


Fig. 5. Plot of point of zero charge of pine leaves.

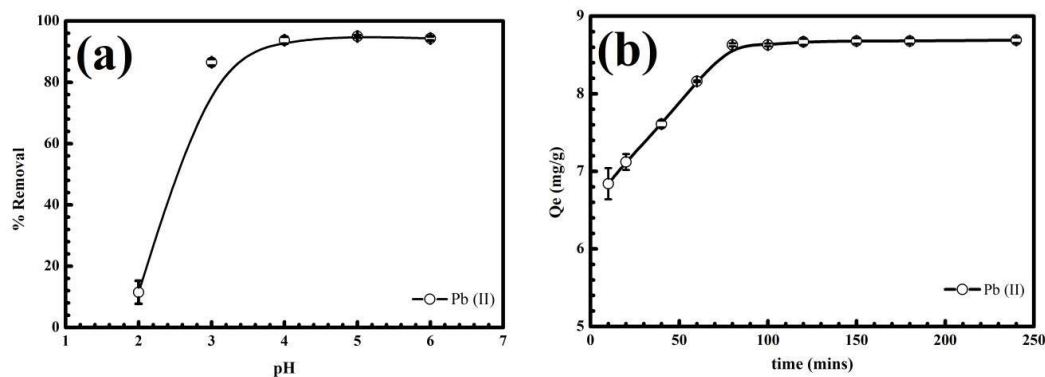


Fig. 6. Effect of pH (a) and adsorption time (b) on the uptake of lead (II) ions (initial concentration of lead (II) solution = 50 mg L⁻¹, adsorbent dose = 0.5 g, temperature = 25°C, shaking speed = 240 rpm, error bar = SD with $n = 3$).

Fig. 6b illustrates the removal of Pb(II) ions from aqueous solution from 10 to 240 min. As can be seen, the amount of absorbed metal ions increases with increasing contact time in the initial stage (0–60 min), then rises in a gradual manner, prior to reach the equilibrium after approximately 90 min for Pb(II).

3.3. CCD experiments and optimization

The experiment program describing the interaction of Pb(II) adsorption capacity and three influential factors are designed by the RSM with CCD. Within the latter, by using the quadratic Eq. (4) with the inputs of pH (A), time (B), concentration (C), and $\pm\alpha$ given in Table 1, we are able to obtain the best fitted equation for the uptake capacity ($Q_e = y$) of Pb(II) as follows

$$Q_e \text{ (mg/g)} = 35.94 + 3.419 \times \text{pH} - 0.08692 \times \text{time} - 0.2674 \times \text{initial concentration} - 0.005875 \times \text{pH} \times \text{time} + 0.01913 \times \text{pH} \times \text{initial concentration} - 0.6677 \times \text{pH}^2 + 0.000704 \times \text{time}^2 + 0.000483 \times \text{initial concentration}^2 \quad (8)$$

In addition, the analysis of variance (ANOVA) has been performed, in which the obtained p and F values are used to evaluate the interaction between the predicted response and adsorption parameters. A p -value less than 0.05 indicates that there is a statistically significant difference between the means at 95% confidential index. The smaller the magnitude of p -value is, the more significant the corresponding coefficient should be considered. Moreover, the fitting quality of the quadratic model is indicated by the coefficient of determination R^2 . According to the statistics shown in Table 3, the obtained high determination coefficient ($R^2 = 0.9703$) shows the good fit of the above model. It means that nearly 97.03% of the response variations can be explained by the quadratic model. On the contrary, the adjusted R^2 value of 0.9436 indicates that approximately 5.6% of the total variations cannot be satisfied with this model. Also, the p -value < 0.0001 obtained in this study confirms the statistical significance of the model with 99.99% confident interval.

The interaction between the model predictions by the quadratic expression is given in Eq. (8) and the experimental

Table 3
ANOVA for the adsorption of Pb(II) onto pine leaves

| Source | Sum of squares | DF | Mean square | F-value | p-value | Comments | |
|---|----------------|----|-------------|---------|----------------------|--------------------------|---------|
| Model | 13.50 | 9 | 1.50 | 36.33 | <0.0001 ^s | Std. Dev. | 0.2032 |
| A-pH | 0.3191 | 1 | 0.3191 | 7.73 | 0.0194 ^s | Mean | 16.89 |
| B-Time (t) | 1.68 | 1 | 1.68 | 40.81 | <0.0001 ^s | C.V. % | 1.20 |
| C-Initial concentration (C ₀) | 1.26 | 1 | 1.26 | 30.57 | 0.0003 ^s | Adjusted R ² | 0.9436 |
| AB | 0.1105 | 1 | 0.1105 | 2.68 | 0.1329 ⁿ | Predicted R ² | 0.7687 |
| AC | 1.17 | 1 | 1.17 | 28.36 | 0.0003 ^s | R ² | 0.9703 |
| BC | 0.0018 | 1 | 0.0018 | 0.0436 | 0.8388 ⁿ | Adeq precision | 24.5910 |
| A ² | 6.42 | 1 | 6.42 | 155.64 | <0.0001 ^s | | |
| B ² | 1.14 | 1 | 1.14 | 27.69 | 0.0004 ^s | | |
| C ² | 0.5381 | 1 | 0.5381 | 13.04 | 0.0048 ^s | | |
| Residual | 0.4128 | 10 | 0.0413 | | | | |
| Lack of fit | 0.4121 | 5 | 0.0824 | 603.05 | <0.0001 ^s | | |
| Pure error | 0.0007 | 5 | 0.0001 | | | | |
| Cor total | 13.91 | 19 | | | | | |

Note: ^ssignificant at $p < 0.05$, ⁿinsignificant at $p > 0.05$.

values are presented in Fig. 7. As can be clearly seen from this figure, the fit between the actual and predicted values is quite good because the model predictions are well scattered on either side of the X-Y line.

Figs. 8a, 8b and 8c show the combined effects of factors affected the Pb(II) adsorption capacity. There is a clearly defined pattern on the graph, which means that the interactive effect is insignificant when pH and time (AB) as well as time and initial concentration (BC) are combined together because their p -values are higher than 0.05. However, there is a significant interaction effect of variables in combination with the Pb(II) adsorption capacity. In this case, the first-order effects of A (pH), B (time) and C (initial concentration), the interaction effects of AC (pH vs. initial concentration), and the square effects of A² (pH²), B² (time²), C² (initial concentration²) are the significant terms in the model.

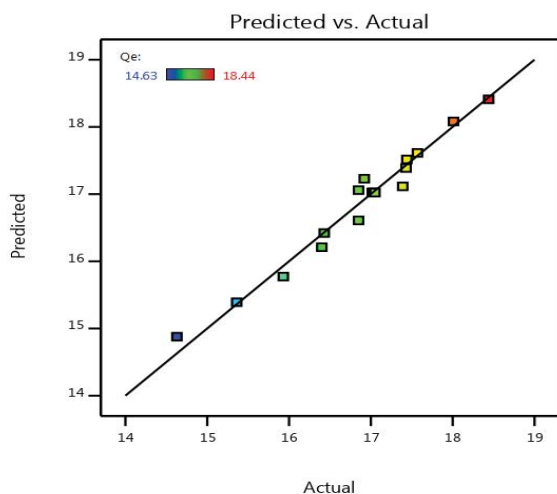


Fig. 7. Quadratic model predictions and experimental values.

By using the numerical optimization, a desirable value for each input factor and response can be selected. In this study, the input variables were given by some specific values, whereas the response was designed to achieve a maximum. Using these conditions, the maximum achieved Pb(II) removal efficiency was 18.17 mg/g (Fig. 9) at an initial pH of 5.08, adsorption time of 110 min and Pb(II) initial concentration of 210 mg/L.

3.4. Adsorption isotherm models

Adsorption isotherm models have been utilized to explain interaction between adsorbents and adsorbates during the uptake as well as to determine maximum adsorption capacity of the adsorbent for Pb(II) ions [1]. Plots of these models are shown in Fig. 10 and non-linear parameters are presented in Table 4. From the calculated results, it is clear that Sips model gives the best fit for the adsorption of Pb(II) ions because of its highest R² and smallest RMSE and c² values. The maximum monolayer Pb(II) adsorption capacity Q_{max} estimated from Langmuir model are 31.04 mg/g suggesting that this material can be used to remove Pb(II) better than some other biomaterials (Table 5).

The n values from Freundlich model is less than 10 and more than 1, which confirms the heterogeneity of the adsorbent surface. In addition, the heat (b_T) and energy (E) of the adsorption calculated from Temkin and Dubinin–Radushkevich are less than 8 kJ mol⁻¹. The above results show that the uptake of Pb(II) follows a physical process [1,15].

3.5. Adsorption kinetics

A kinetic study of adsorption is necessary as it provides the information about the adsorption mechanism, which is crucial for the practicality of the process. Fig. 11 shows plots of kinetic models and Table 6 presents the non-linear parameters of these models. According to the statistics, it

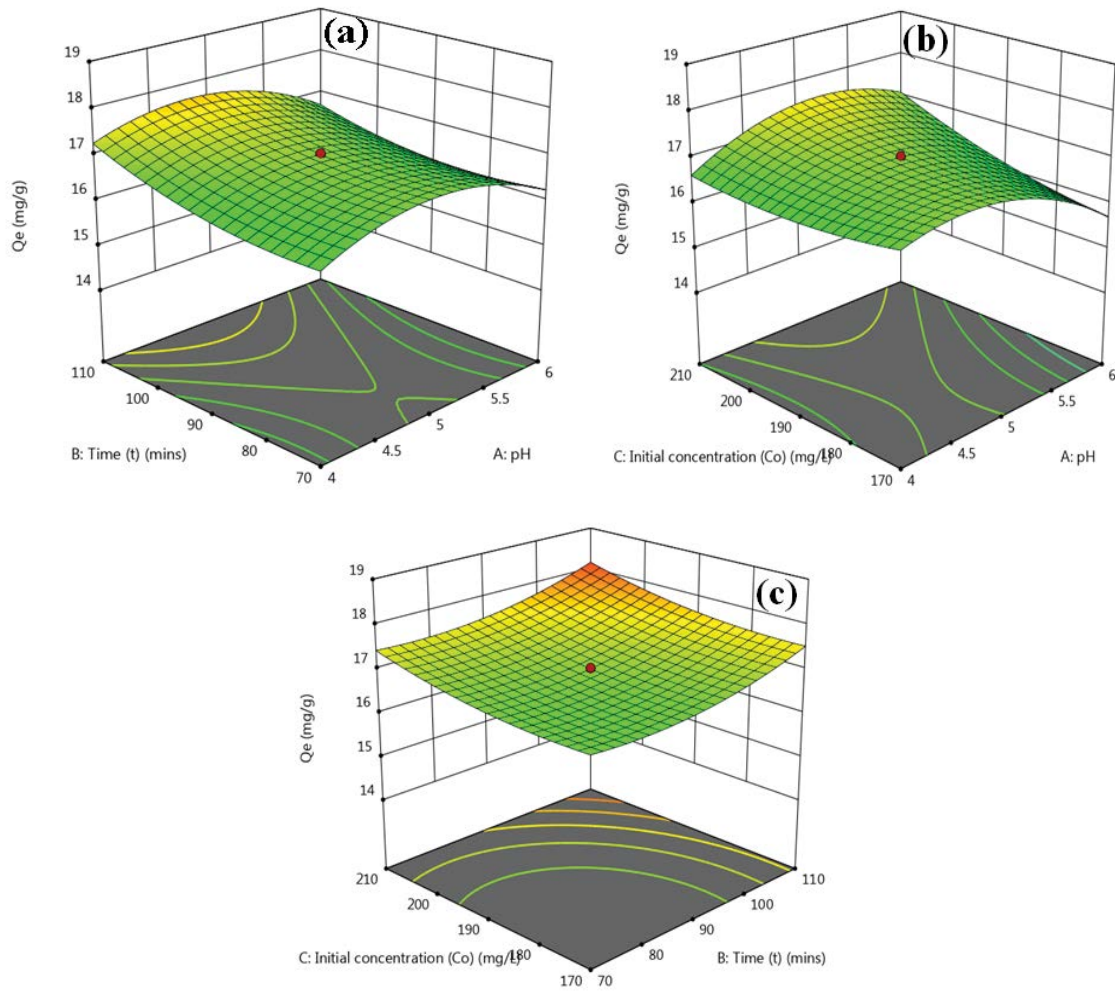


Fig. 8. 3D response surface graphs for combined effect on Pb(II) adsorption capacity of (a) pH and adsorption time; (b) pH and initial concentration; (c) adsorption time and initial concentration.

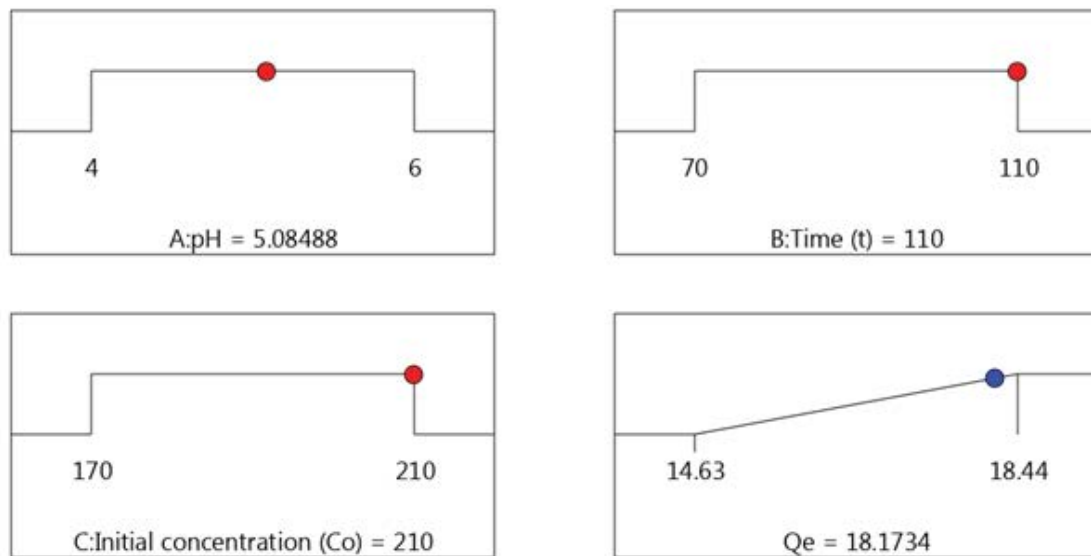


Fig. 9. Desirability ramp for the optimization of the response and the variables.

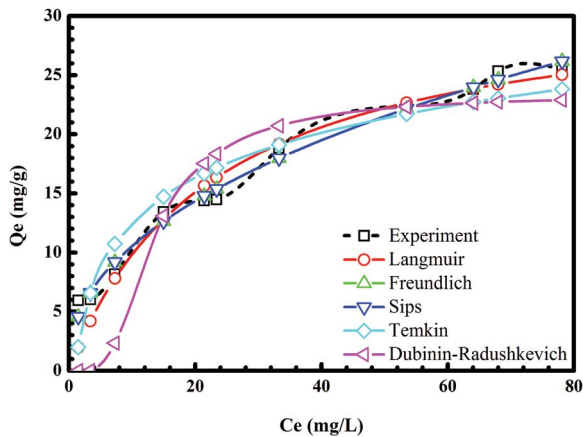


Fig. 10. Plots of non-linear isotherm models for the adsorption of Pb(II) onto *Pinus kesiya* leaves.

Table 4
Non-linear isotherm parameters

| Isotherm models | Non-linear parameters | |
|------------------------|-----------------------|---------|
| Langmuir | K_L | 0.0470 |
| | Q_m (mg/g) | 31.04 |
| | RMSE | 1.219 |
| | R^2 | 0.9721 |
| | χ^2 | 1.923 |
| Freundlich | n | 2.15 |
| | K_F | 3.53 |
| | RMSE | 0.6411 |
| | R^2 | 0.9925 |
| | χ^2 | 0.2892 |
| Sips | Q_s | 3.21 |
| | α_s | 4.3E-02 |
| | β_s | 0.5730 |
| | RMSE | 0.6167 |
| | R^2 | 0.9928 |
| Temkin | χ^2 | 0.2664 |
| | K_T (L/mg) | 0.8190 |
| | b_T (kJ/mol) | 0.4460 |
| | RMSE | 1.616 |
| | R^2 | 0.9509 |
| Dubinin - Radushkevich | χ^2 | 2.579 |
| | Q_{D-R} (mol/g) | 21.84 |
| | β | 15.89 |
| | E (kJ/mol) | 0.18 |
| | RMSE | 3.645 |
| | R^2 | 0.7501 |
| | χ^2 | 15.25 |

is obvious that the experimental data of Pb(II) adsorption kinetics can be described by the Elovich model due to its highest R^2 and smallest RMSE and c^2 values. The results of

Table 5
Comparison of sorption capacity of Pb(II) with some bio materials

| Materials | pH | Q_m (mg/g) | Ref. |
|--|-----|--------------|------------|
| Barley straw | 6.0 | 23.20 | [26] |
| <i>Cucumis sativus</i> (cucumber) peel | 5.0 | 28.25 | [26] |
| Coconut tree sawdust | 6.0 | 25.00 | [21] |
| Eggshell | 6.0 | 90.90 | [21] |
| Sugarcane bagasse | 6.0 | 21.28 | [21] |
| Coconut coir | 5.0 | 37.04 | [27] |
| Durian tree sawdust | 5.0 | 20.37 | [27] |
| Pine leaves | 5.0 | 31.04 | This study |

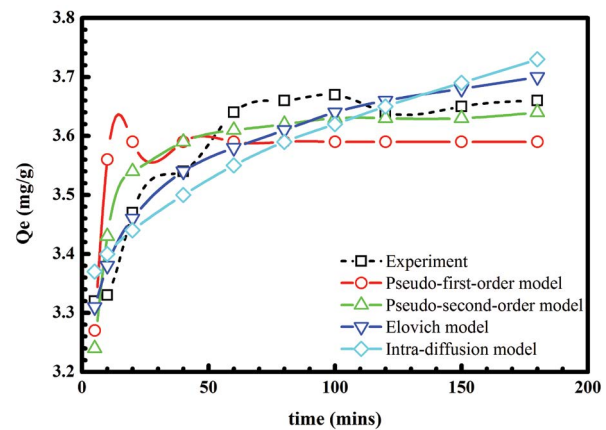


Fig. 11. Plots of kinetic models for the adsorption of Pb(II) onto *P. kesiya* leaves.

the present study confirm that the surface of *P. kesiya* leaves is a heterogeneous system which is positively correlated with Fig. 2. Additionally, a decrease in the intensities of specific peaks without the shift recorded in Fig. 4 demonstrated that the primary mechanism of the adsorption of Pb(II) onto *P. kesiya* leaves is electrostatic attraction [14].

Although the intraparticle diffusion model developed by Weber and Morris was not applied to determine the surface properties of *P. kesiya* leaves, it was utilized to identify the diffusion mechanism in the adsorption process. Fig. 12 shows that there are two stages in the uptake of Pb^{2+} ions on *P. kesiya* leaves. In addition, the value of C calculated from this model, which is not zero, illustrates that the sorption follows not only the intraparticle diffusion but also two or more different diffusion mechanisms [1]

3.6. Thermodynamic studies

Calculation of thermodynamic parameters is also used to reaffirm the nature of the adsorption process. These parameters include Gibbs free energy change (ΔG^0), enthalpy change (ΔH^0) and entropy change (ΔS^0). The Gibbs free energy change can be determined from the following equation:

$$\Delta G^0 = -RT \ln K_C \tag{9}$$

where T is temperature in Kelvin, R is the gas constant having a value of $8.314 \text{ J mol}^{-1} \text{ K}^{-1}$, and K_C is the equilibrium constant calculated from the Langmuir constant based on the following equation [28]:

$$KC = KL \times 207 \times 10^3 \times 55.5 \tag{10}$$

Table 6
Non-linear kinetic model parameters

| Kinetics models | Parameters | |
|-----------------------------|---|----------|
| Pseudo-first order kinetic | C_o (mg/L) | 88 |
| | $q_{e(\text{exp})}$ (mg/g) | 8.80 |
| | $q_{e(\text{cal})}$ (mg/g) | 8.44 |
| | k_1 (min ⁻¹) | 0.1416 |
| | RMSE | 0.4711 |
| | R^2 | 0.5872 |
| | χ^2 | 0.2643 |
| Pseudo-second order kinetic | $q_{e(\text{cal})}$ (mg/g) | 8.83 |
| | k_2 (g mg ⁻¹ min ⁻¹) | 0.0310 |
| | RMSE | 0.2574 |
| | R^2 | 0.8767 |
| | χ^2 | 0.0801 |
| Elovich kinetics | α | 1.15E+03 |
| | β | 1.424 |
| | RMSE | 0.1940 |
| | R^2 | 0.9300 |
| | χ^2 | 0.0405 |
| Intraparticle diffusion | K_p | 0.1689 |
| | C | 6.620 |
| | RMSE | 0.3084 |
| | R^2 | 0.8231 |
| | χ^2 | 0.1038 |

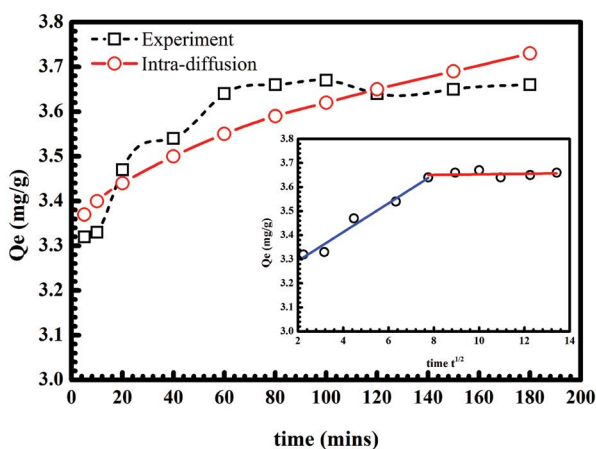


Fig. 12. Intra-diffusion model for the adsorption of Pb (II) onto *P. kesiyaa* leaves.

From the Van't Hoff equation, the thermodynamic parameters such as enthalpy, entropy and Gibbs free energy were calculated using equations [29]:

$$\Delta G^0 = \Delta H^0 - T\Delta S^0 \tag{11}$$

The relationship between the equilibrium constant K_L and enthalpy were determined by the equation of Clausius–Clapeyron:

$$\ln K_c = \frac{\Delta S^0}{R} - \frac{\Delta H^0}{RT} \tag{12}$$

The change in enthalpy and entropy were calculated from the slope and intercept of the linear plot $\ln K_C$ vs. $1/T$ (Fig. 13). The calculated values of these parameters are tabulated in Table 7.

As can be seen from the table, ΔG^0 has a negative value at different temperatures and the negative value from -38.66 to $-41.23 \text{ kJ mol}^{-1}$ at the temperature range studies, indicating that the adsorption process takes place automatically and the adsorption rate increases with increasing temperature [30].

The results for ΔH^0 and ΔS^0 were found to be 0.24 kJ mol^{-1} and $128.41 \text{ J mol}^{-1}$, respectively. The positive of ΔH^0 value suggests that adsorption process was endothermic in nature [31].

In addition to that, the positive value of entropy (ΔS^0) can be assigned to increase randomness at the solid–liquid interface during the adsorption of Pb(II) onto dried plants.

4. Conclusion

The adsorption of Pb(II) ions onto *P. kesiyaa* leaves affected by various physico-chemical parameters, such as contact time, pH and initial concentration of the metal ions, was optimized by RSM with CCD. ANOVA analysis shows a significant interaction effect of variables in combination with the Pb(II) adsorption capacity. The optimal condition for the Pb(II) maximum removal is the pH of 5.08, adsorption time of 110 min and Pb(II) initial concentration of 210 mg/L. The Pb(II) maximum adsorption capacity (Q_{max}) estimated

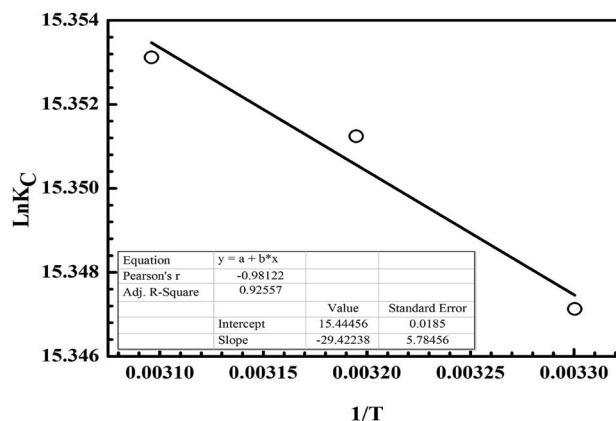


Fig. 13. Plot of $\ln K_C$ vs. $1/T$.

Table 7
Thermodynamic parameters

| T | K_L | K_C | $\ln K_C$ | $1/T$ | ΔH (kJ mol ⁻¹) | ΔS (J mol ⁻¹) | ΔG (kJ mol ⁻¹) |
|-----|---------|---------|-----------|--------|------------------------------------|-----------------------------------|------------------------------------|
| 303 | 0.0470 | 4625646 | 15.35 | 0.0033 | 0.24 | 128.41 | -38.66 |
| 313 | 0.04718 | 4644721 | 15.35 | 0.0032 | | | -39.95 |
| 323 | 0.04726 | 4653441 | 15.35 | 0.0031 | | | -41.23 |

from the Langmuir isotherm model was 31.04 mg/g. The Elovich kinetic model offers the best fit experimental data ($R^2 = 0.9300$), which confirms the heterogeneous system of this material. Based on the results of thermodynamic studies, it can be concluded that adsorption Pb(II) ions onto *P. kesiya* followed physical process. This study demonstrates that *P. kesiya* leaves are promising adsorbent for the removal of Pb(II) ions from aqueous solution owing to its high adsorption capacity and, especially, naturally and abundantly available at a low cost.

References

- [1] V.-P. Dinh, N.-C. Le, L.A. Tuyen, N.Q. Hung, V.-D. Nguyen, N.-T. Nguyen, Insight into adsorption mechanism of lead(II) from aqueous solution by chitosan loaded MnO₂ nanoparticles, *Mater. Chem. Phys.*, 207 (2018) 294–302.
- [2] T. Şahan, F. Erol, Ş. Yılmaz, Mercury(II) adsorption by a novel adsorbent mercapto-modified bentonite using ICP-OES and use of response surface methodology for optimization, *Microchem. J.*, 138 (2018) 360–368.
- [3] R.R. Karri, M. Tanzifi, M. Tavakkoli Yarak, J.N. Sahu, Optimization and modeling of methyl orange adsorption onto polyaniline nano-adsorbent through response surface methodology and differential evolution embedded neural network, *J. Environ. Manage.*, 223 (2018) 517–529.
- [4] V. Kumar Gupta, S. Agarwal, M. Asif, A. Fakhri, N. Sadeghi, Application of response surface methodology to optimize the adsorption performance of a magnetic graphene oxide nanocomposite adsorbent for removal of methadone from the environment, *J. Colloid Interface. Sci.*, 497 (2017) 193–200.
- [5] V. Javanbakht, S.M. Ghoreishi, Application of response surface methodology for optimization of lead removal from an aqueous solution by a novel superparamagnetic nanocomposite, *Adsorpt. Sci. Technol.*, 35 (2016) 241–260.
- [6] Y. Bulut, Z. Baysal, Removal of Pb(II) from wastewater using wheat bran, *J. Environ. Manage.*, 78 (2006) 107–113.
- [7] A. Adeyemo, A. Egbedina, K. Adebawale, B. Olu-owolabi, Removal of cadmium (II) from aqueous solutions by pinecone biochar, *Res. J. Chem. Environ. Sci.*, 2 (2015) 98–102.
- [8] E. Missanjo, D. Kapira, Storage conditions and period effects on quality of *Pinus kesiya* seeds from Malawi, *Sch. Acad. J. Biosci.*, 3 (2015) 315–319.
- [9] A. Sisodia, M. Padhi, A.K. Pal, K. Barman, A.K. Singh, Seed Priming on Germination, Growth and Flowering in Flowers and Ornamental Trees, In: A. Rakshit, H.B. Singh, Eds., *Advances in Seed Priming*. Singapore: Springer Singapore; 2018, p. 263–288.
- [10] N.S. El-Gendy, H.R. Madian, S.S.A. Amr, Design and optimization of a process for sugarcane molasses fermentation by *Saccharomyces cerevisiae* using response surface methodology, *Int. J. Microbiol.*, 2013 (2013) 9.
- [11] U. Shafique, A. Ijaz, M. Salwan, Wu Zaman, N. Jamil, R. Rehman, A. Javaid, Removal of arsenic from water using pine leaves, *J. Taiwan Inst. Chem. Eng.*, 43 (2012) 256–263.
- [12] T. Tran, Q. Bui, T. Nguyen, V. Ho, L.G. Bach, Application of response surface methodology to optimize the fabrication of ZnCl₂-activated carbon from sugarcane bagasse for the removal of Cu²⁺, *Water Sci. Technol.*, 75 (2017) 2047–2055.
- [13] K.Y. Foo, B.H. Hameed, Insights into the modeling of adsorption isotherm systems, *Chem. Eng. J.*, 156 (2010) 2–10.
- [14] H. Tran, S.-J. You, T.V. Nguyen, H.-P. Chao, Insight into adsorption mechanism of cationic dye onto biosorbents derived from agricultural wastes, *Chem. Eng. Commun.*, 204 (2017) 1020–1036.
- [15] V.-P. Dinh, N.-C. Le, V.-D. Nguyen, N.-T. Nguyen, Adsorption of zinc (II) onto MnO₂/CS composite: equilibrium and kinetic studies, *Desal. Wat. Treat.*, 58 (2017) 427–434.
- [16] Q.T. Trinh, B.K. Chethana, S.H. Mushrif, Adsorption and reactivity of cellulosic aldoses on transition metals, *J. Phys. Chem. C*, 119 (2015) 17137–17145.
- [17] P.N. Amaniampong, A. Karam, Q.T. Trinh, K. Xu, H. Hiraio, F. Jérôme, G. Chatel, Selective and catalyst-free oxidation of D-glucose to D-glucuronic acid induced by high-frequency ultrasound, *Sci. Rep.*, 7 (2017) 40650.
- [18] P.N. Amaniampong, Q.T. Trinh, K. Li, S.H. Mushrif, Y. Hao, Y. Yang, Porous structured CuO-CeO₂ nanospheres for the direct oxidation of cellobiose and glucose to gluconic acid, *Catal. Today*, 306 (2018) 172–182.
- [19] M.T. Yagub, T.K. Sen, H.M. Ang, Equilibrium, kinetics, and thermodynamics of methylene blue adsorption by pine tree leaves, *Water Air Soil Pollut.*, 223 (2012) 5267–5282.
- [20] P.N. Amaniampong, Q.T. Trinh, J.J. Varghese, R. Behling, S. Valange, S.H. Mushrif, F. Jérôme, Unraveling the mechanism of the oxidation of glycerol to dicarboxylic acids over a sonchemically synthesized copper oxide catalyst, *Green Chem.*, 20 (2018) 2730–2741.
- [21] W.P. Putra, A. Kamari, S.N.M. Yusoff, C.F. Ishak, A. Mohamed, N. Hashim, M.I. Isa, Biosorption of Cu(II), Pb(II) and Zn(II) ions from aqueous solutions using selected waste materials: adsorption and characterisation studies, *J. Encapsul. Adsorpt. Sci.*, 4 (2014) 25–35.
- [22] N.E. Wanja, J. Murungi, A.H. Ali, R. Wanjaw, Efficacy of adsorption of Cu (II), Pb (II) and Cd (II) ions onto acid activated watermelon peels biomass from water, *Int. J. Sci. Res.*, 5 (2016) 671–679.
- [23] X. Wang, L. Wang, Y. Wang, R. Tan, X. Ke, X. Zhou, J. Geng, H. Hou, M. Zhou, Calcium sulfate hemihydrate whiskers obtained from flue gas desulfurization gypsum and used for the adsorption removal of lead, *Crystals*, 7 (2017) 270.
- [24] K.J. Powell, P.L. Brown, R.H. Byrne, T. Gajda, G. Heffer, A.K. Leuz, S. Sjöberg, H. Wanner, Chemical speciation of environmentally significant metals with inorganic ligands. Part 3: The Pb²⁺, OH⁻, Cl⁻, CO₃²⁻, SO₄²⁻, and PO₄³⁻ systems (IUPAC Technical Report), 81 (2009) 2425–2476.
- [25] S. Asgarzadeh, R. Rostamian, E. Faez, A. Maleki, H. Daraei, Biosorption of Pb(II), Cu(II), and Ni(II) ions onto novel lowcost *P. eldarica* leaves-based biosorbent: isotherm, kinetics, and operational parameters investigation, *Desal. Wat. Treat.*, 57 (2016) 14544–14551.
- [26] E. Pehlivan, T. Altun, S. Parlayıcı, Utilization of barley straws as biosorbents for Cu²⁺ and Pb²⁺ ions, *J. Hazard. Mater.*, 164 (2009) 982–986.
- [27] S.N.M. Yusoff, A. Kamari, W.P. Putra, C.F. Ishak, A. Mohamed, N. Hashim, M.I. Isa, Removal of Cu(II), Pb(II) and Zn(II) ions from aqueous solutions using selected agricultural wastes: adsorption and characterisation studies, *J. Environ. Protect.*, 5 (2014) 289–300.
- [28] X. Zhou, X. Zhou, The unit problem in the thermodynamic calculation of adsorption using the Langmuir equation, *Chem. Eng. Commun.*, 201 (2014) 1459–1467.

- [29] N.K. Mondal, A. Samanta, S. Dutta, S. Chattoraj, Optimization of Cr (VI) biosorption onto *Aspergillus niger* using 3-level Box-Behnken design: equilibrium, kinetic, thermodynamic and regeneration studies, *J. Genet. Eng. Biotechnol.*, 15 (2017) 151–160.
- [30] T. Mahmood, S. Din, A. Naeem, S. Tasleem, A. Alum, S. Mustafa, Kinetics, equilibrium and thermodynamics studies of arsenate adsorption from aqueous solutions onto iron hydroxide, *J. Ind. Eng. Chem.*, 20 (2014) 3234–3242.
- [31] M. Chiban, G. Carja, G. Lehtu, F. Sinan, Equilibrium and thermodynamic studies for the removal of As (V) ions from aqueous solution using dried plants as adsorbents, *Arab. J. Chem.* 9 (2016) S988–S999.